nature chemical biology

C_3-symmetric peptide scaffolds are functional mimetics of trimeric CD40L

Sylvie Fournel[1], Sébastien Wieckowski[1], Weimin Sun[1,5], Nathalie Trouche[1], Hélène Dumortier[1], Alberto Bianco[1], Olivier Chaloin[1], Mohammed Habib[2], Jean-Christophe Peter[1], Pascal Schneider[3], Bernard Vray[2], René E Toes[4], Rienk Offringa[4], Cornelis J M Melief[4], Johan Hoebeke[1] & Gilles Guichard[1]

Interaction between CD40, a member of the tumor necrosis factor receptor (TNFR) superfamily, and its ligand CD40L, a 39-kDa glycoprotein, is essential for the development of humoral and cellular immune responses[1,2]. Selective blockade or activation of this pathway provides the ground for the development of new treatments against immunologically based diseases[3,4] and malignancies[5,6]. Like other members of the TNF superfamily, CD40L monomers self-assemble around a threefold symmetry axis to form noncovalent homotrimers that can each bind three receptor molecules[7,8]. Here, we report on the structure-based design of small synthetic molecules with C_3 symmetry that can mimic CD40L homotrimers. These molecules interact with CD40, compete with the binding of CD40L to CD40, and reproduce, to a certain extent, the functional properties of the much larger homotrimeric soluble CD40L. Architectures based on rigid C_3-symmetric cores may thus represent a general approach to mimicking homotrimers of the TNF superfamily.

CD40L is expressed mainly on activated T cells, whereas its cognate receptor, CD40, is constitutively expressed on dendritic cells (DC), macrophages and B cells. The engagement of CD40 by its ligand contributes to regulation of B cell proliferation, immunoglobulin production, immunoglobulin class switching, germinal center formation and development of B cell memory[1]. Moreover, CD40-CD40L interaction has an essential role in cellular immune response in which CD40 ligation activates DCs, 'licensing' them to present antigen to cytotoxic T cells by increasing MHC and costimulatory molecule expression and by producing high levels of IL-12, a T cell–stimulating cytokine[9–11]. Antibodies against CD40 with agonist activity have been used to increase immune response in infectious diseases[12,13] and in cancer immunotherapy[5,6]. All of these results underscore the important therapeutic applications that could emerge from the development of small-molecule CD40 agonists.

Although ligand-induced dimerization is a general mechanism for activating receptors of cytokines and growth factors[14], signaling through receptors of the TNFR superfamily strongly relies on the formation of stoichiometrically defined C_3-symmetric complexes[7]. The structures of several TNF family members in complex with their cognate receptors show that each ligand homotrimer interacts with three monomeric receptor chains[7,15,16]. The geometry of the resulting 3:3 hexameric complex is favorable to the formation of an internal 3:3 signaling complex between the intracellular tail of the receptor and transduction proteins, ultimately activating downstream effector pathways[7].

Despite the difficulty in identifying small molecules that can disrupt protein-protein interactions, synthetic agonists of homodimeric cytokine receptors have been reported[17,18]. The ability of these molecules to dimerize cell-surface receptors is a major determinant of their effector functions[19]. In the present study, we have developed CD40L mimetics by integrating threefold symmetry as a design principle. We reasoned that such trimeric architectures, besides providing the correct geometry for receptor trimerization, could also achieve tight binding to CD40 with receptor-binding elements of low surface areas (for example, small peptides)[20,21]. Although the CD40L-CD40 interaction has not been determined at the atomic level, a model of the complex built using the X-ray structure of CD40L and a homology model of CD40 (ref. 22) has provided the basis for the structure-based design of trivalent ligands (**Fig. 1a**). Both rigid, flat macrocyclic (D,L-α-hexapeptide and β^3-tripeptide) and flexible branched C_3-symmetric scaffolds have been considered as core structures to distribute receptor-binding elements with geometry and distances that could match those of the CD40L homotrimer (**Fig. 1b**). Five 'hot spot' residues in CD40L (namely, Lys143, Tyr145, Tyr146 (in the AA″ loop), Arg203 (in the DE loop) and Gln220 (in the F strand)) have been previously identified using a combination of molecular modeling and site-directed mutagenesis[22,23]. Mutations of these CD40L surface residues markedly affect binding to CD40. On the basis of these considerations, the small CD40-interacting

[1]UPR 9021 CNRS, Immunologie et Chimie Thérapeutiques, Institut de Biologie Moléculaire et Cellulaire, 15 rue René Descartes, F-67084 Strasbourg Cedex, France. [2]Laboratoire d'Immunologie Expérimentale (CP 615), Faculté de Médecine, Université Libre de Bruxelles, 808 Route de Lennik, 1070 Brussels, Belgium. [3]Department of Biochemistry, University of Lausanne, Ch. des Boveresses 155, CH-1066 Epalinges. [4]Leiden University Medical Center, Department of Immunohaematology and Blood Transfusion, Albinusdreef 2, E3-Q, Postbox 9600, 2300 RC, Leiden, The Netherlands. [5]Present address: Institute of Biological Science and Technology, Beijing Jiaotong University, 3 Shang Yuan Cun, Haidian District, 100044 Beijing, China. Correspondence should be addressed to G.G. (G.Guichard@ibmc.u-strasbg.fr) or S.F. (s.fournel@ibmc.u-strasbg.fr).

Received 7 July; accepted 17 October; published online 6 November 2005; doi:10.1038/nchembio746

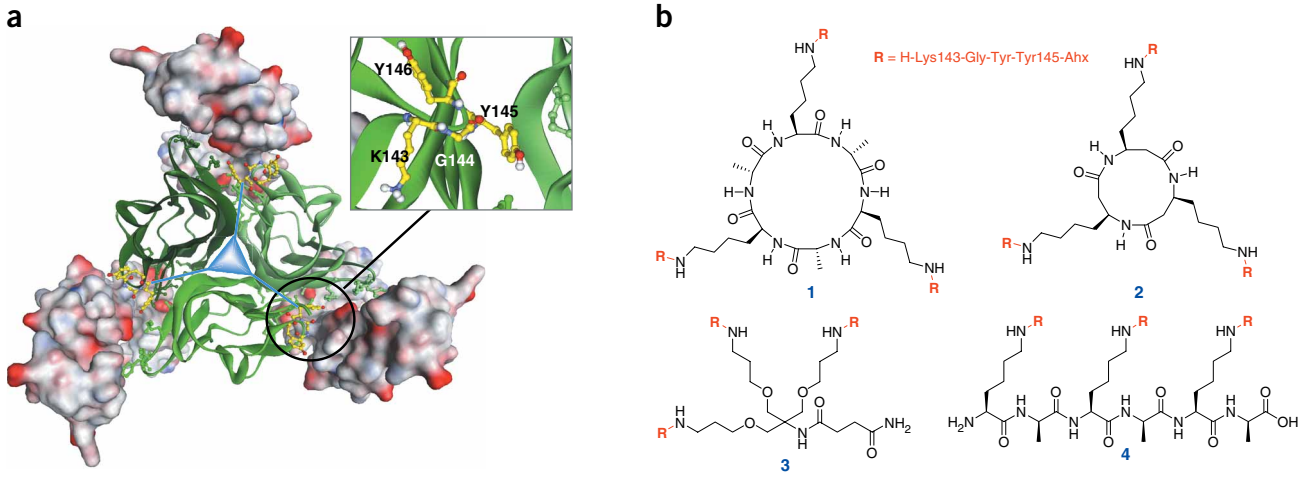

Figure 1 Synthetic C_3-symmetric CD40L mimetics. (**a**) Model of the 3:3 complex between CD40 (surface representation) and CD40L (ribbon) viewed down the C_3 axis[22] and schematic representation of the structure-based approach to the design of CD40L homotrimer mimetics. The distance between the center of the CD40L homotrimer and the CD40 binding surface is ~21 Å. Box shows a magnified view of the polar CD40-binding surface and the hot spot region Lys143–Tyr146 selected as the CD40 binding motif. (**b**) Trimeric compounds **1**–**4** were synthesized by fragment coupling of the fully protected Boc-Lys(Boc)-Gly-Tyr(O*t*Bu)-Tyr(O*t*Bu)-Ahx-OH pentapeptide to the corresponding cores in solution as described for **1** in the **Supplementary Methods**. Boc, *t*-butoxycarbonyl; O*t*Bu: *t*-butyl ether.

region Lys143-Gly-Tyr-Tyr146 of CD40L was selected as a CD40-binding motif and tethered via an amino hexanoic acid (Ahx) residue spacer to the central core structures to give compounds **1**–**3** (**Fig. 1b**).

To determine whether the resulting trimeric ligands interact with CD40, we performed a series of surface plasmon resonance (SPR) experiments using a recombinant human CD40-mouse immunoglobulin (hCD40:mIg) immobilized on the sensor chip via an anti-mouse Fc or 5C3 an anti-human CD40 monoclonal antibody (anti-hCD40 mAb; **Fig. 2** and **Supplementary Fig. 1** online). We mixed a fixed amount of recombinant human soluble CD40L tethered to a mouse CD8 tail (hCD40L:CD8) with increasing concentrations of synthetic molecules, and we then performed inhibition SPR by injecting those samples over the sensor surface. Compounds with the CD40 binding motif appended to a macrocyclic core (namely, **1** and **2**) competed with binding of hCD40L:CD8 to CD40 in a concentration-dependent manner with a median inhibitory

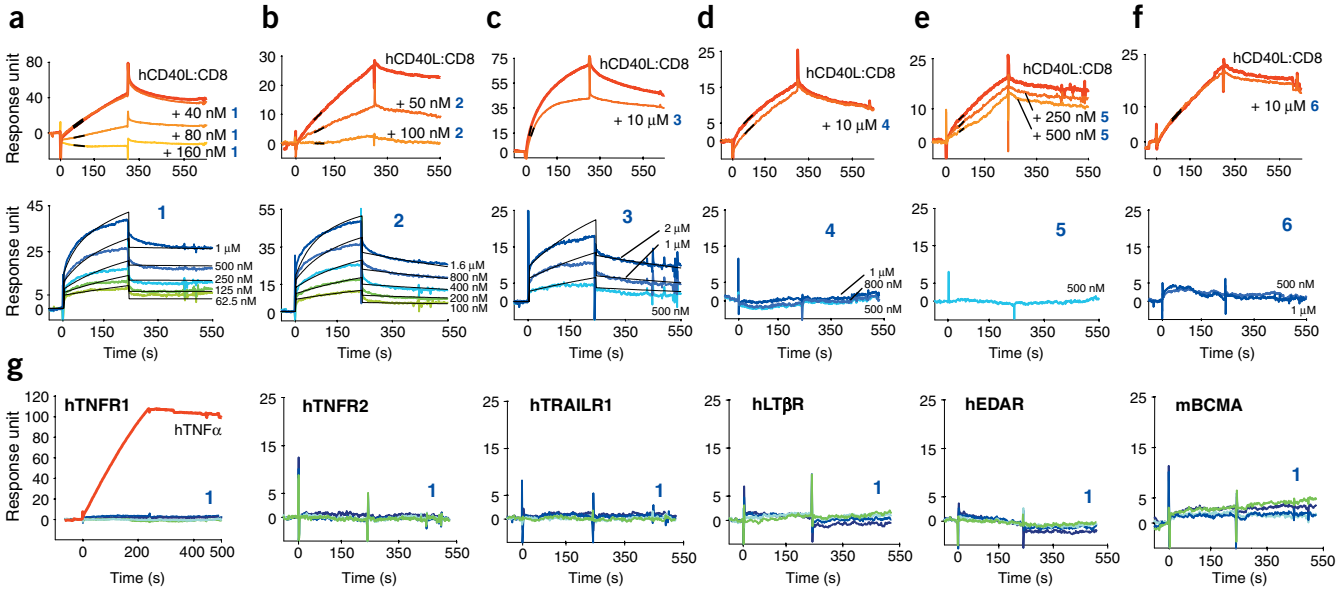

Figure 2 SPR experiments using hCD40:mIg. (**a**–**f**) Upper row shows inhibition of CD40-binding by SPR. Ligands **1**–**6** were tested for their capacity to inhibit the binding of soluble hCD40L:CD8 to CD40. The tendency of **5** to aggregate under SPR conditions prevented analyses of SPR data for concentrations >500 nM. Thick lines on the inhibition sensorgrams correspond to sections of the linear part of the kinetics (v_0) relevant to calculations of the percentage inhibition. Lower row illustrates direct binding to CD40, as shown by SPR. The binding data for **1** and **2** were fitted using a trivalent binding model (**Supplementary Table 1**). (**g**) Compound **1** (125 nM, 250 nM, 500 nM, 1 μM) did not bind to a subset of TNFR family members (~1,000 RU), as shown by SPR. As a control, binding of TNFα to TNFR1 is shown in the leftmost panel.

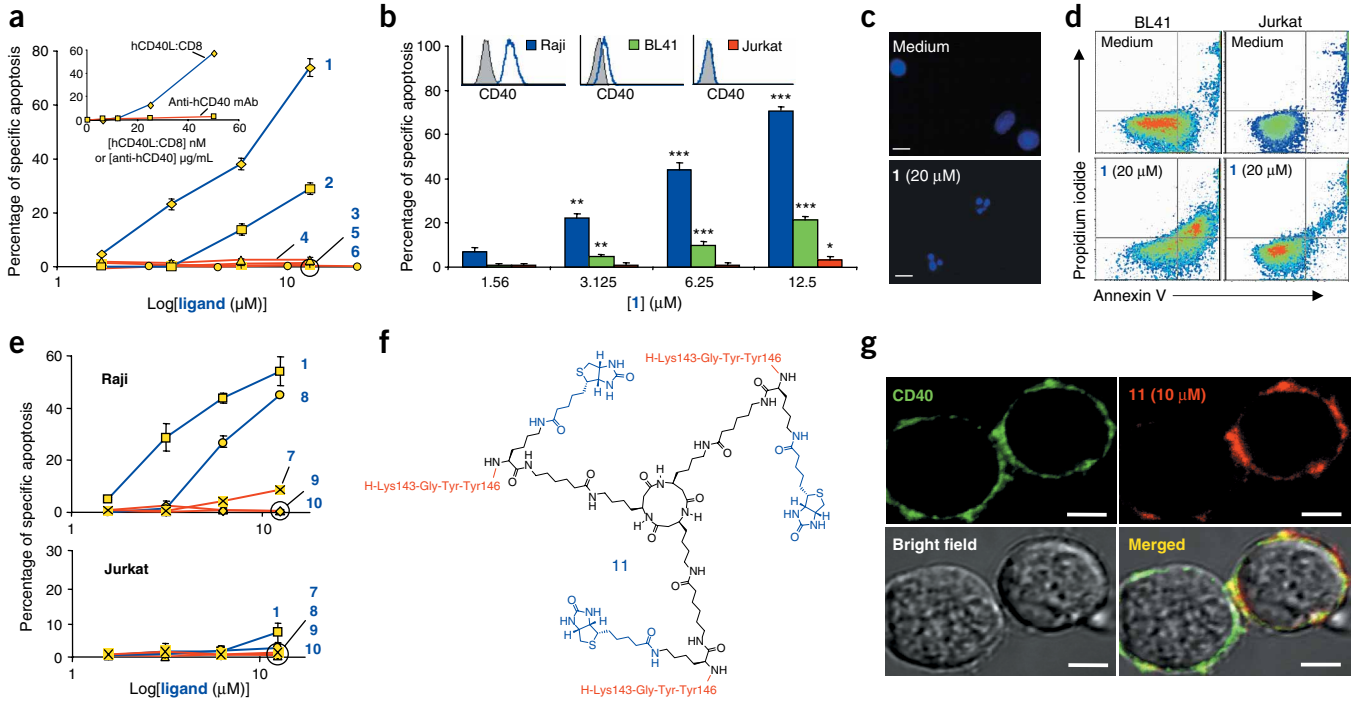

Figure 3 CD40L mimetics induce apoptosis of Burkitt lymphoma cells and colocalize with endogenous CD40. (**a**,**b**) Induction of apoptosis studied by the decrease of $\Delta\psi_m$, as detected by a reduction of $DiOC_6(3)$ dye uptake. (**a**) Effect of **1**–**6** on Raji cells. hCD40L:CD8 and anti-hCD40 mAb 5C3 are shown in inset. (**b**) Effect of **1** on cell lines expressing various levels of CD40. Results are expressed as the average (± s.e.m.) of three independent experiments. $^*P > 0.01$; ** $0.01 > P > 0.005$; *** $P < 0.005$ (Student's *t*-test). Insets show relative cell number as a function of CD40 expression (as measured by mean fluorescence intensity (MFI)). (**c**) Characteristic nucleus fragmentation of apoptotic BL41 cells treated by **1** observed after DAPI staining using epifluorescence microscopy. (**d**) Detection of phosphatidylserine externalization by flow cytometry after colabeling with annexin V-FITC and propidium iodide after treatment with **1**. (**e**) Scanning single–amino acid substitutions within the CD40 binding motif of **1**. Effect of **7** (K143G), **8** (G144A), **9** (Y145A), and **10** (Y146A) measured as in **a** and compared with **1**. (**f**) Structure of compound **11**, a biotinylated variant of **2**. (**g**) Analysis of colocalization of **11** and anti-CD40 mAb (5C3) by confocal microscopy on Raji cells. Scale bars, 5 µm. Pearson's correlation: $R_r = 0.47$; overlap coefficient: $R = 0.91$.

concentration (IC_{50}) of 78 nM and 50 nM, respectively (**Fig. 2a**,**b**). In contrast, **4,** a linear variant of **1** (**Fig. 2d**), the cyclic D,L-α-hexapeptide core structure of **1** (R = H, **5**; **Fig. 2e**) and the monomeric peptide H-Lys-Gly-Tyr-Tyr-Ahx-OH (**6**; **Fig. 2f**) did not inhibit CD40L binding and therefore served as valuable negative controls. Branched **3** only partially blocked binding of CD40L (20% inhibition at a concentration of 10 µM; **Fig. 2c**). We further investigated interaction of our synthetic molecules with CD40 by direct SPR binding experiments. Compounds **1**, **2** and, to a lesser extent, **3** bound to CD40 in this assay (**Fig. 2a–c** and **Supplementary Fig. 1**). Although the binding of the three molecules could be fitted to a simple monovalent binding model, analysis of SPR sensorgrams using a trivalent binding model gave a better fit for **1** and **2** with χ^2 values (which describe the closeness of the fit) of 1.34 and 0.97, respectively (**Supplementary Table 1** online). This is consistent with the rigid trimeric nature of the chemical CD40 ligands and the dense distribution of the receptor at the surface of the flexible dextran matrix, which could facilitate the formation of tetrameric complexes. The specificity of synthetic mimetics for CD40 is supported by the absence of binding of **1** to other TNFR family members (human TNFR1, TNFR2, LTβR, TRAILR1, EDAR and mouse BCMA, **Fig. 2g**).

To establish whether CD40L mimetics **1** and **2** display effector function(s), we used different cell-based assays with soluble CD40L as a positive control. The first test was based on the property of CD40-positive human Burkitt lymphoma cells to undergo apoptosis upon CD40 engagement[24]. Like hCD40L:CD8, but unlike anti-hCD40 mAb 5C3, compounds **1** and **2** induced a dose-dependent apoptosis of Burkitt lymphoma cells (maximal after 16 h of incubation) as measured by the decrease of the mitochondrial membrane potential ($\Delta\psi_m$; **Fig. 3a**,**b**), morphology criteria after DAPI staining (**Fig. 3c**), and detection of phosphatidylserine expression (by annexin V staining; **Fig. 3d**). The percentage of apoptosis correlated with CD40 expression (**Fig. 3b**). Neither control compounds **4**–**6**, which did not interact with CD40, nor branched **3**, induced apoptosis (**Fig. 3a**), indicating that the ligand architecture markedly influences both the CD40 binding capacity and downstream effector functions, and that distribution of the binding motif in a radial fashion is preferred. Furthermore, singly substituting alanine or glycine for each residue in the CD40 binding sequence in **1** established the importance of Lys143, Tyr145 and Tyr146 residues in both determining binding of **1** (**Supplementary Fig. 2** online) to CD40 and inducing apoptosis of B lymphoma cells (**Fig. 3e**).

To verify that CD40L mimetics target CD40 at the surface of lymphoma cells, we synthesized **11,** a biotinylated C_3-symmetric variant of **2** (**Fig. 3f**). Like **1** and **2**, compound **11** bound to CD40 in SPR experiments and induced Burkitt lymphoma cell apoptosis (**Supplementary Fig. 3** online). Using colocalization experiments with the anti-hCD40 mAb 5C3 (**Fig. 3g**) and flow cytometry staining (**Supplementary Fig. 3**), we found that compound **11** binds to CD40 at the surface of CD40-positive cells but was not detected at the surface of CD40-negative cells. Notably, binding of compound **11** was markedly reduced at 4 °C (**Supplementary Fig. 3**), suggesting that membrane fluidity is required for optimal CD40 binding.

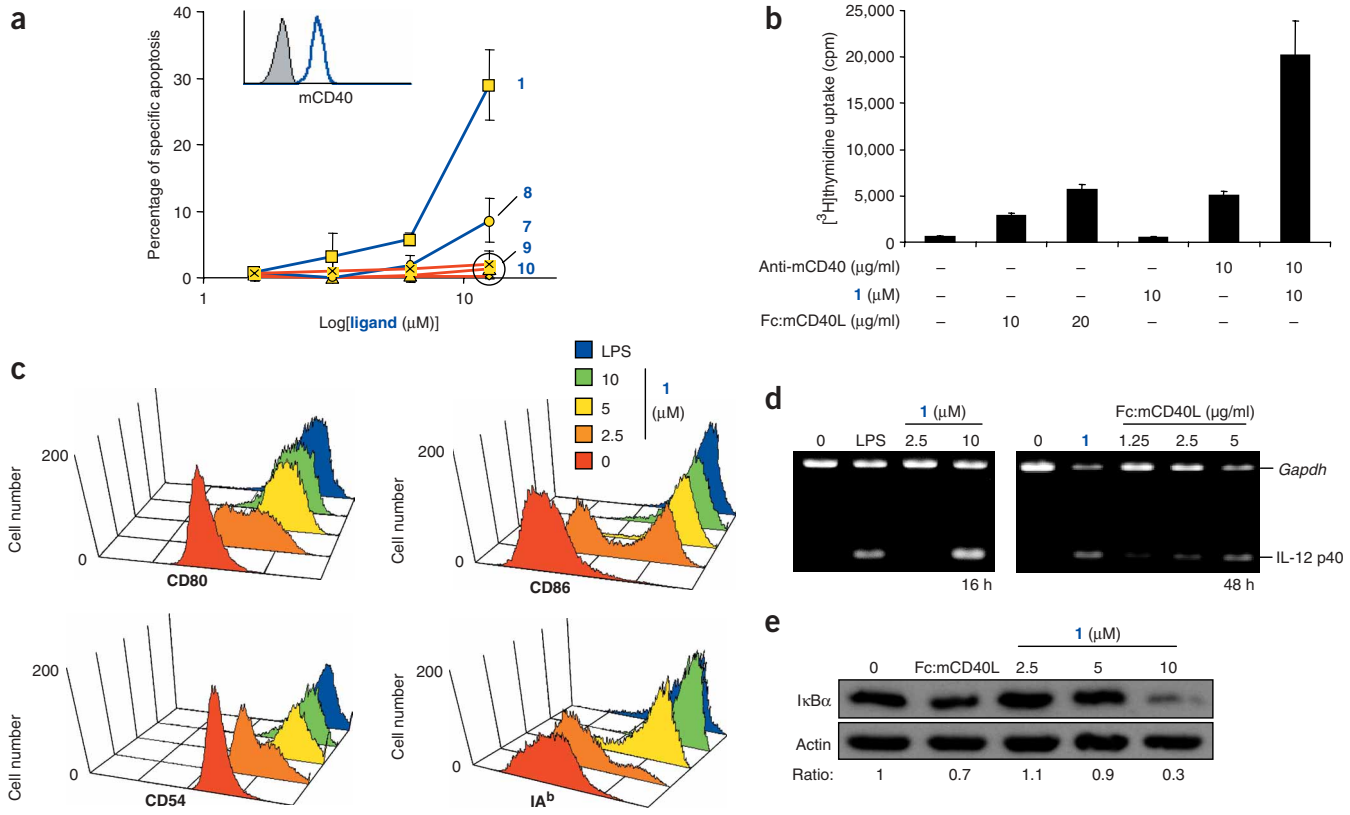

Figure 4 Effect of **1** on various mouse cells. (**a**) Induction of apoptosis of mouse A20 lymphoma cells after treatment with **1**, measured as in **Figure 3a**. Analogs **7**–**10** included as controls. Inset shows relative cell number as a function of CD40 expression (as measured by MFI). (**b**) Synergy by **1** of the proliferative response induced by an agonistic anti-mouse CD40 antibody. Results are expressed as average c.p.m. ± s.d. of two different experiments. (**c**–**e**) Compound **1** induces maturation of the mouse dendritic cell line D1 and activation of the NF-κB pathway. As a control, 10 μg ml^{-1} LPS was used. (**c**) Expression of maturation markers, as measured by flow cytometry after 48 h of treatment with **1**. (**d**) Comparative RT-PCR detection of IL-12 p40 mRNA in D1 cells, with mRNA expression of the housekeeping gene *Gapdh* as a control. (**e**) Analysis by immunoblotting of IκBα expression in D1 cells. As a control, actin expression was evaluated under the same conditions. Intensity ratio between IκBα and actin is shown below each lane.

Compound **1** also induced apoptosis of mouse CD40–expressing B lymphoma cells (**Fig. 4a**). Human and mouse CD40L sequences share 77% identity, and the sequence of the CD40-interacting loop region Lys143-Gly-Tyr-Tyr146 is conserved between both species. This result may suggest that ligands based on this conserved binding motif could also mimic mouse CD40L.

To study the effect of CD40L mimetics on nontransformed cells, purified splenic mouse B cells were treated with CD40L mimetics as well as with a mouse recombinant CD40L (Fc:mCD40L). Whereas Fc:mCD40L at high dose and anti-mouse CD40 mAb 3/23 induced B cell proliferation, compound **1** at 10 μM had no effect on B cell proliferation. However, in a manner analogous to soluble CD40L (ref. 25), **1** at 10 μM synergized the proliferation induced by the agonistic anti-mCD40 mAb 3/23 (**Fig. 4b**). These results underscore the difference between SPR binding data and cellular assays. On one hand, one can assume that the distribution of CD40 molecules at the surface of the chip significantly differs from that at the cell surface, both qualitatively (in terms of flexibility, accessibility and fluidity) and quantitatively (in terms of density). On the other hand, our findings are in agreement with a number of studies showing that receptor trimerization in the TNFR family is not always sufficient to induce effective signaling and that higher order oligomers are required[24–27]. Although synthetic ligands based on trimeric architectures probably bound CD40 on B cells by recruiting more than one receptor chain, they might fail to generate sufficient CD40 oligomerization to reach the activation threshold.

Finally, we investigated the capacity of CD40L mimetics to induce DC maturation by using the mouse DC line D1 which matures upon CD40 ligation[28]. Like Fc:mCD40L, compound **1** (5–10 μM) but not compounds **4**–**6**, induced upregulation of MHC and costimulatory molecule expression (**Fig. 4c** and **Supplementary Fig. 4** online) as well as production of interleukin (IL)-12, as visualized by IL-12 p40 mRNA (**Fig. 4d**) and protein (**Supplementary Fig. 4**) expression. At higher doses (>20 μM), maturation was accompanied by cell death. It is noteworthy that the maturation was not decreased in the presence of polymyxin B, an inhibitor of lipopolysaccharide (LPS) LPS activity, thus ruling out the possibility of a CD40-independent, LPS-mediated maturation of D1 cells (**Supplementary Fig. 4**). Moreover, compound **1** activated the NF-κB pathway[29] as shown by the increased degradation of the IκBα protein (**Fig. 4e**), suggesting that CD40L mimetics and natural CD40L use the same signaling pathway.

Our results indicate that relatively small (<3 kDa) synthetic trivalent architectures can mimic *in vitro* the effects of noncovalent signaling protein homotrimers and suggest the possibility of using small CD40 ligands to amplify immune responses *in vivo*. Extension of the approach to additional TNF members might prove useful to modulate TNFR functions in various pathological situations.

METHODS

CD40L mimetics. For details of preparation and characterization of **1** and **5** as well as alanine-substituted analogues **7–10**, see **Supplementary Methods** online and **Supplementary Figure 5** online. Trimeric ligands **1–4** were highly soluble in water (>20 mg ml^{-1}). For sample preparation, ligands were dissolved in water at a concentration of 1 mM before dilution to the indicated concentrations in appropriate buffer or medium.

SPR analysis. BIAcore 3000 (Biacore AB) was used to evaluate the binding of CD40L mimetics to CD40. Flow cells of a Biacore AB CM5 Sensor Chip (Research Grade, Biacore AB) were precoated with a rabbit polyclonal antibody directed against mouse immunoglobulin (RAM-Ig, Biacore AB) or with a goat antibody directed against human immunoglobulin (GAH-Ig, Jackson, ImmunoResearch Laboratories) using amine coupling at 30 μg ml^{-1} in 10 mM acetate buffer, pH 5.5, according to the manufacturer's protocol. The chip was then flushed with 1 M ethanolamine hydrochloride, pH 8.5 (Biacore AB), and 50 mM HCl to eliminate unbound antibody. Generally ~10,000 resonance units (RU) of RAM-Ig or GAH-Ig were obtained after immobilization. Biosensor assays were performed at 25 °C with HBS-EP buffer (10 mM HEPES, pH 7.4, containing 0.15 M NaCl, 3.4 mM EDTA and 0.005% (v/v) P20 surfactant (Biacore AB)) as running buffer. We captured soluble human CD40-mIg fusion protein (hCD40:mIg; Ancell Corporation), mouse anti-huCD40 antibody (Pharmingen), other TNFR:Fc fusion proteins, and LG11-2 (an IgG2a mouse monoclonal antibody directed against H2B histone used as irrelevant control) on individual flow cells at a flow rate of 5 μl min^{-1} and at a concentration allowing equivalent protein mass binding.

Binding of CD40L to CD40. hCD40L:CD8 (Ancell) was injected at a flow rate of 30 μl min^{-1} over the control channel and the CD40 channel for 5 min and was allowed to dissociate for an additional 5 min. The channels were regenerated for 30 s with 50 mM HCl. Control sensorgrams were subtracted from the CD40 sensorgrams and analyzed by BIAevaluation 4.1 with the 1:1 Langmuir binding model or a trivalent model[30].

Inhibition of CD40L binding to CD40. hCD40L:CD8 fusion protein was injected at 100 nM (**Fig. 2a,b,d–f**) or 200 nM (**Fig. 2c**) under the same conditions at a flow rate of 10 μl min^{-1} in the presence of various concentrations of CD40L mimetics. The IC_{50} was estimated from the decrease in the initial linear association phase.

Direct binding of the CD40L mimetics. CD40L mimetics were injected at different concentrations under the same conditions. The corrected sensorgrams were analyzed by BIAevaluation 4.1 with binding models as indicated in **Supplementary Table 1** online.

Measurement of apoptosis. Cell death was evaluated either by measurement of a decrease in mitochondrial transmembrane potential ($\Delta\psi_m$) associated with a reduction of the cationic dye $DiOC_6(3)$ uptake, as demonstrated by flow cytometry, or by detection of phosphatidylserine externalization by flow cytometry after colabeling with annexin V–FITC and propidium iodide (PI). Results are expressed as percentage of specific apoptosis according to the following formula: percentage specific apoptosis = ((percentage of apoptotic treated cells – percentage of apoptotic control cells) × 100)/(100 – percentage of apoptotic control cells). Full experimental procedures are provided in **Supplementary Methods**.

Cell culture and apoptosis induction. Burkitt lymphoma (BL41 and Raji), Jurkat human T lymphoma, and 3T6 murine fibroblasts were cultured in RPMI 1640 (Cambrex Bioscience) supplemented with 10% heat-decomplemented fetal bovine serum (FBS) and gentamicin (10 μg ml^{-1}). For apoptosis assays, cells (5×10^5 ml^{-1}) were incubated at 37 °C in 24-well plates at the indicated times and concentrations in presence of the various inducers. After incubation, cells were washed with PBS before measurement of apoptosis as described above.

Purification and culture of splenic B cells. Spleens were removed from 5- to 12-week-old BALB/c mice. Splenic B cells were prepared by positive selection using magnetic beads coated with anti-CD19 mAb (MACS, Milteny Biotech). This fraction contained more than 95% $B220^+$ cells. B cells (3×10^6 ml^{-1}) were then cultured in RPMI 1640 medium supplemented with 10% heat-decomplemented FBS, gentamicin (10 μg ml^{-1}), 25 mM HEPES and 10 μM β-mercaptoethanol in the presence of CD40L mimetics, or Fc:mCD40L and/or anti-mouse CD40 mAb (3/23). Cells were pulsed with [^{3}H]thymidine (1 μCi per well; ICN) during the last 20 h of culture, and [^{3}H]thymidine uptake was measured after 72 h using a Matrix 9600 direct β counter (Packard). The results are given as the arithmetic mean of thymidine uptake expressed as c.p.m.

Culture and maturation of D1 cells. D1 cells were cultured in nontreated plastic dishes in IMDM medium (Cambrex) supplemented with 10% heat-decomplemented FBS, penicillin (100 international units (IU) ml^{-1}), 10 μM β-mercaptoethanol, 2 mM L-glutamine and 30% (v/v) of supernatant of NIH/3T3 cells as a source of granulocyte-monocyte colony-stimulating factor (GM-CSF). For the maturation assay, 2×10^5 cells ml^{-1} were cultured for 48 h. Fresh medium containing the various inducers was then added. After various times of incubation, supernatants were collected to measure IL-12 production, and cells were washed with cold PBS and then harvested with 2 ml of PBS containing 2 mM EDTA. After centrifugation, cells were resuspended in cold PBS and analyzed for cell surface phenotyping by flow cytometry or were used for RT-PCR and western blotting analysis as described in **Supplementary Methods**.

Flow cytometry, confocal microscopy, western blot, RT-PCR and IL-12 measurement. Classical procedures were used. Full experimental procedures are provided in **Supplementary Methods**.

Note: Supplementary information is available on the Nature Chemical Biology website.

ACKNOWLEDGMENTS

We thank J.-P. Briand and S. Muller for support; J. Mutterer for assistance with confocal microscopy; N. Bonnefoy-Berard and M. Flacher for providing Burkitt lymphoma cells and M. Monestier for providing LG11-2 mAb. This work was supported by the Centre National de la Recherche Scientifique, the Ministère de la Recherche (ACI Jeunes Chercheurs), La Ligue contre le Cancer, Région Alsace and the Agence Nationale de Recherches contre le SIDA. S.W. was supported by a grant from the Ministère de la Recherche. W.S. was supported by the Ministère de la Recherche and the Fondation pour la Recherche Médicale. N.T. was supported by La Ligue Contre le Cancer.

AUTHOR CONTRIBUTION STATEMENT

S.F. and S.W. contributed equally to this work. W.S. and N.T. contributed equally to this work.

COMPETING INTERESTS STATEMENT

The authors declare that they have no competing financial interests.

Published online at http://www.nature.com/naturechemicalbiology/
Reprints and permissions information is available online at http://npg.nature.com/reprintsandpermissions/

1. van Kooten, C. & Banchereau, J. CD40–CD40 ligand. *J. Leukoc. Biol.* **67**, 1–17 (2000).
2. Diehl, L. *et al.* The role of CD40 in peripheral T cell tolerance and immunity. *J. Mol. Med.* **78**, 363–371 (2000).
3. Howard, L.M. *et al.* Mechanisms of immunotherapeutic intervention by anti-CD40L (CD154) antibody in an animal model of multiple sclerosis. *J. Clin. Invest.* **103**, 281–290 (1999).
4. Kirk, A.D. *et al.* Treatment with humanized monoclonal antibody against CD154 prevents acute renal allograft rejection in nonhuman primates. *Nat. Med.* **5**, 686–693 (1999).
5. Diehl, L. *et al.* CD40 activation *in vivo* overcomes peptide-induced peripheral cytotoxic T-lymphocyte tolerance and augments anti-tumor vaccine efficacy. *Nat. Med.* **5**, 774–779 (1999).
6. Sotomayor, E.M. *et al.* Conversion of tumor-specific CD4+ T-cell tolerance to T-cell priming through *in vivo* ligation of CD40. *Nat. Med.* **5**, 780–787 (1999).
7. Bodmer, J.-L., Schneider, P. & Tschopp, J. The molecular architecture of the TNF superfamily. *Trends Biochem. Sci.* **27**, 19–26 (2002).
8. Karpusas, M. *et al.* 2 Å crystal structure of an extracellular fragment of human CD40 ligand. *Structure* **3**, 1031–1039 (1995).
9. Schoenberger, S.P., Toes, R.E., van der Voort, E.I., Offringa, R. & Melief, C.J. T-cell help for cytotoxic T lymphocytes is mediated by CD40–CD40L interactions. *Nature* **393**, 480–483 (1998).
10. Bennett, S.R. *et al.* Help for cytotoxic-T-cell responses is mediated by CD40 signalling. *Nature* **393**, 478–480 (1998).
11. Cella, M. *et al.* Ligation of CD40 on dendritic cells triggers production of high levels of interleukin-12 and enhances T cell stimulatory capacity: T-T help via APC activation. *J. Exp. Med.* **184**, 747–752 (1996).

12. Chaussabel, D. *et al.* CD40 ligation prevents Trypanosoma cruzi infection through interleukin-12 upregulation. *Infect. Immun.* **67**, 1929–1934 (1999).
13. Edelmann, K.H. & Wilson, C.B. Role of CD28/CD80–86 and CD40/CD154 costimulatory interactions in host defense to primary herpes simplex virus infection. *J. Virol.* **75**, 612–621 (2001).
14. Heldin, C.-H. Dimerization of cell surface receptors in signal transduction. *Cell* **80**, 213–223 (1995).
15. Liu, Y. *et al.* Ligand-receptor binding revealed by the TNF family member TALL-1. *Nature* **423**, 49–56 (2003).
16. Hymowitz, S.G. *et al.* Structures of APRIL-receptor complexes: like BCMA, TACI employs only a single cysteine-rich domain for high affinity ligand binding. *J. Biol. Chem.* **280**, 7218–7227 (2005).
17. Wrighton, N.C. *et al.* Small peptides as potent mimetics of the protein hormone erythropoietin. *Science* **273**, 458–464 (1996).
18. Cwirla, S.E. *et al.* Peptide agonist of the thrombopoietin receptor as potent as the natural cytokine. *Science* **276**, 1696–1699 (1997).
19. Whitty, A. & Borysenko, C.W. Small molecule cytokine mimetics. *Chem. Biol.* **6**, R107–R118 (1999).
20. Mammen, M., Choi, S.-K. & Whitesides, G.M. Polyvalent interactions in biological systems: implications for design and use of multivalent ligands and inhibitors. *Angew. Chem. Int. Edn Engl.* **37**, 2754–2794 (1998).
21. Kiessling, L.L., Gestwicki, J.E. & Strong, L.E. Synthetic multivalent ligands in the exploration of cell-surface interactions. *Curr. Opin. Chem. Biol.* **4**, 696–703 (2000).
22. Singh, J. *et al.* The role of polar interactions in the molecular recognition of CD40L with its receptor CD40. *Protein Sci.* **7**, 1124–1135 (1998).
23. Bajorath, J. *et al.* Analysis of gp39/CD40 interactions using molecular models and site-directed mutagenesis. *Biochemistry* **34**, 9884–9892 (1995).
24. Tong, A.W. *et al.* CD40 ligand-induced apoptosis is Fas-independent in human multiple myeloma cells. *Leuk. Lymphoma* **36**, 543–558 (2000).
25. Pound, J.D. *et al.* Minimal cross-linking and epitope requirements for CD40-dependent suppression of apoptosis contrast with those for promotion of the cell cycle and homotypic adhesions in human B cells. *Int. Immunol.* **11**, 11–20 (1999).
26. Schneider, P. *et al.* Conversion of membrane-bound Fas (CD95) ligand to its soluble form is associated with downregulation of its proapoptotic activity and loss of liver toxicity. *J. Exp. Med.* **187**, 1205–1213 (1998).
27. Haswell, L.E., Glennie, M.J. & Al-Shamkhani, A. Analysis of the oligomeric requirement for signaling by CD40 using soluble multimeric forms of its ligand, CD154. *Eur. J. Immunol.* **31**, 3094–3100 (2001).
28. Schuurhuis, D.H. *et al.* Immature dendritic cells acquire CD8(+) cytotoxic T lymphocyte priming capacity upon activation by T helper cell-independent or -dependent stimuli. *J. Exp. Med.* **192**, 145–150 (2000).
29. O'Sullivan, B.J. & Thomas, R. CD40 ligation conditions dendritic cell antigen-presenting function through sustained activation of NF-kappaB. *J. Immunol.* **168**, 5491–5498 (2002).
30. Lortat-Jacob, H., Chouin, E., Cusack, S. & van Raaij, M.J. Kinetic analysis of adenovirus fiber binding to its receptor reveals an avidity mechanism for trimeric receptor-ligand interactions. *J. Biol. Chem.* **276**, 9009–9015 (2001).